CLSM method for the dynamic observation of pH change within polymer matrices for oral delivery

Article

pubs.acs.org/Biomac

CLSM Method for the Dynamic Observation of pH Change within Polymer Matrices for Oral Delivery

Michael T. Cook,[†,‡] Teedah Saratoon,[§] George Tzortzis,[∥] Alexander Edwards,[‡] Dimitris Charalampopoulos,*[,†] and Vitaliy V. Khutoryanskiy*[,‡]

[†]Department of Food and Nutritional Sciences and [‡]Reading School of Pharmacy, University of Reading, Reading, RG6 6AD, United Kingdom

[§]Department of Medical Physics and Bioengineering, University College London, Gower Street, London, WC1E 6BT, United Kingdom

[∥]Clasado Research Services Ltd., Science and Technology Centre, University of Reading, Earley Gate, Whiteknights Road, Reading, RG6 6BZ, United Kingdom

Supporting Information

ABSTRACT: If acid-sensitive drugs or cells are administered orally, there is often a reduction in efficacy associated with gastric passage. Formulation into a polymer matrix is a potential method to improve their stability. The visualization of pH within these materials may help better understand the action of these polymer systems and allow comparison of different formulations. We herein describe the development of a novel confocal laser-scanning microscopy (CLSM) method for visualizing pH changes within polymer matrices and demonstrate its applicability to an enteric formulation based on chitosan-coated alginate gels. The system in question is first shown to protect an acid-sensitive bacterial strain to low pH, before being studied by our technique. Prior to this study, it has been claimed that protection by these materials is a result of buffering, but this has not been demonstrated. The visualization of pH within these matrices during exposure to a pH 2.0 simulated gastric solution showed an encroachment of acid from the periphery of the capsule, and a persistence of pHs above 2.0 within the matrix. This implies that the protective effect of the alginate-chitosan matrices is most likely due to a combination of buffering of acid as it enters the polymer matrix and the slowing of acid penetration.

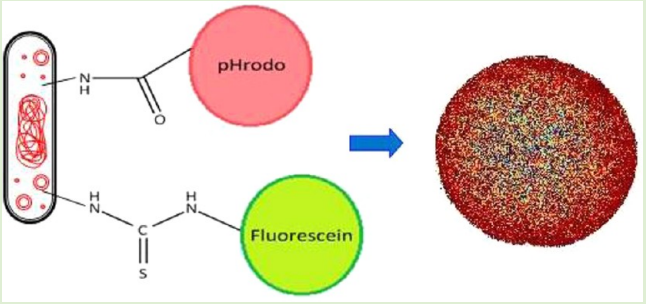

INTRODUCTION

When delivering acid sensitive bioactives orally there are often problems associated with the low pH of the stomach adversely affecting the administration. Examples of such bioactives include acid-labile drugs, such as penicillin G,[1] antigens,[2] or microorganisms, such as live bacterial vaccines or probiotic bacteria.[3,4] Although the entrapment of these species in enteric dosage forms has been shown to improve drug stability,[5] or reduce cell death,[4,6] the mechanisms of protection are usually hypothesized and very rarely demonstrated or quantified dynamically. These mechanisms are likely to be either a result of the polymer's insolubility in acid, halting penetration of acid into the polymer matrix, or the buffering capacity of the polymers in the formulation raising the pH inside the matrices to a level which is no longer harmful to the encapsulated material.[7,8]

When an enterically formulated bioactive is taken orally there is only a short period of transition through the esophagus (around 10−14 s).[9] Upon entry to the stomach, a lower pH is encountered, due to hydrochloric acid secretion by parietal cells found in the gastric epithelium.[10] The pH of the gastric juices is highly variable; it can reach as low as pH 1[11] in fasted patients and as high as pH 5 in a fed state.[12] These gastric secretions also include some enzymes which assist in the digestion of foods, the most abundant of which is the proteolytic enzyme, pepsin. Transit through the stomach varies due to a range of factors including age, gender, and meal volume[13] but usually occurs within 1−2 h after ingestion of the meal.[14] The enteric formulation will then pass from the stomach and into the lower digestive tract where pH rises to near neutral, at which point it will deliver the bioactive.

To this date, there are limited studies describing the visualization of the pH distribution in pharmaceutical formulations.[15] These focus on the measurement of pH within PLGA microspheres,[16−19] PLGA films,[20,21] tablets,[22] and within pellets.[23] For example, Fu et al.[17] have entrapped SNARF (seminaphthorhodafluor)/NERF (carboxy-2,7-dimethyl-3-hydroxy-6-*N*-ethylaminospiro [isobenzofuran-1(3*H*),9-(9*H*)-

Received: October 9, 2012
Revised: January 9, 2013
Published: January 9, 2013

xanthen]-3-one)-dextran dyes into hollow PLGA microspheres to measure the pH change within the particles as the polymers biodegrade. While this method is fit for their purpose, it cannot be used for a highly porous polymer matrix system, when there is the possibility of diffusion out of the matrix or where there would be direct contact between the dye and polymers. Indeed, more recent studies by Liu et al. and Li et al.[16,18] describe confocal visualization of pH change within PLGA microparticles containing acid-sensitive proteins using pH-responsive dyes. This study encounters a fluorescence quenching effect due to the interaction of the dye with entrapped proteins. To resolve this issue, an estimation of quenching was required and additional experimentation was needed to validate this. A study by Pygall et al.[22] measured the pH in HPMC tablets during exposure to 0.1 M HCl containing 0.5% (v/v) universal pH indicator. This allowed for the visualization of the hydration of the pellet and gave an indication of the pH in those regions. While providing useful information in that study, this method is limited in that the dye must diffuse in from the periphery of the formulation, meaning that pH visualization is not possible in regions were no indicator is present.

In this study we have developed a method that is, to our knowledge, the only currently available reliable technique for accurately visualizing the pH in hydrated polymer matrices dynamically and which can be applied to a variety of porous systems. This method has been developed in order to better understand the behavior of hydrogel systems containing bioactives during exposure to low pH. In brief, a Gram-positive *Bifidobacterium* strain was labeled with two pH-sensitive fluorophores, which could be independently excited. The pixel intensity ratio of images taken by confocal laser-scanning microscopy (CLSM) can be color coded, which allows the visualization of pH within formulations during exposure to acidic solutions. This method could be applied to any system in which the bacteria may be suspended within a matrix. The use of these microorganisms as a carrier for the dyes means that issues, such as fluorescence quenching, surrounding excipient−dye interactions are removed, thus, widening the application over other methods[16−18,23] that require the entrapment, or uptake, of a dye into the formulation. Another advantage of using bacterial cells as a model bioactive is that bacteria are of a large enough size (>1 μm) that they will not diffuse or "reptate" out of all but the most porous formulations. This improves on previous methods that rely on small dye molecules being retained by the polymer matrix, which is not often the case in systems which are submerged in liquid. The method presented in this study serves as a means of investigating the protective effect of enteric formulations under these conditions. Additionally, both of the dyes used are nonselective, so can be used for various microbes.

The strain of bacteria used, *B. breve*, is a rod-shaped, nonmotile anaerobe that naturally inhabits the human intestine. Like all *Bifidobacterium* strains, it is gram-positive as a result of the thick layer of peptidoglycan constituting its cell wall. In addition to this, *B. breve* produces polysaccharides upon its surface that form a bacterial capsule.[24] The acid sensitivity of these cells arises mainly from the denaturing of proteins within the cell at lowered cytoplasmic pH. These proteins constitute part of the cell's structure and give it some enzymatic activity.[25] Thus, damaging these proteins contributes to the death of the cell.

One formulation which has been shown to protect acid-sensitive bacteria, such as *Bifidobacterium* strains, is the ionic alginate microencapsulation system.[7,8,26−33] This method has been shown to greatly reduce cell death during exposure to gastric pHs,[7,8] and that the subsequent coating of the alginate matrix with the cationic polysaccharide chitosan has improved the bacteria's survival even further.[8,34] Though a buffering effect has been attributed as the cause of protection,[7,8] this claim has not been substantiated by experimentation. Herein a technique is developed in order to understand the change in pH within this alginate-chitosan system better.

MATERIALS

Bifidobacterium breve. NCIMB 8807 (*B. breve*) was purchased from the National Collections of Industrial Food and Marine Bacteria (Aberdeen, U.K.). Alginate (19−40 kDa), fluorescein isothiocyanate (FITC), and low molecular-weight chitosan (103 kDa, degree of deacetylation: 85.6%) were purchased from Sigma-Aldrich (Gillingham, U.K.). pHrodo succinimidyl ester was purchased from Invitrogen (California, U.S.A.). Wilkins-Chalgren (WC) anaerobe agar and phosphate-buffered saline (PBS) were purchased from Oxoid (U.K.). Alginate was purified by microfiltration (0.45 μm sartorius filter) before use; all other reagents were used without further purification. Materials other than alginate and chitosan were sterilized by autoclaving; alginate and chitosan were sterilized by microfiltration.

METHODS

Viability of *B. breve* at pH 2−7. *B. breve* was streaked onto WC agar plates from a previously prepared cell bank and allowed to grow anaerobically (48 h, 37 °C). After growth, an aliquot of the bacteria was used to inoculate tryptone−phytone−yeast (TPY) broth (10 mL) and the culture incubated (22 h, 37 °C) with shaking to late log phase; during this time, the cells grew to ∼9 log(CFU)/mL. The cell suspension was then divided into aliquots (1 mL) and centrifuged (11000 rpm, 5 min) before resuspending the cells into TPY (1 mL) that was adjusted to a variety of pHs (1.0, 2.0, 2.3, 2.6, 3.0, 4.0, 5.0, 6.0, and 7.0) using 1 M HCl. These samples were incubated for 1 h at 37 °C and enumerated by serial dilution in PBS and spreading onto WC agar plates before anareobic incubation (48 h, 37 °C). During incubation, each viable cell present on the plate produced one colony. From this, the total number of viable cells could then be calculated by the multiplication of colony numbers by the dilution factor used. Colonies produced were white and circular with a region of translucency around the edges. Those colonies that did not appear as such were not counted.

Survival of Alginate and Alginate-Chitosan Encapsulated *B. breve* During Simulated Gastrointestinal Passage. *B. breve* was grown as before and centrifuged (3200 rpm, 10 min, 4 °C). The supernatant was removed and the cells resuspended in 2% (w/v) alginate solution. This polymer/cell solution (1 mL) was extruded through a 21G needle into 0.05 M $CaCl_2$ (50 mL) and allowed to harden (30 min). After this period, the capsules were removed by filtration. For chitosan-coated capsules, the alginate encapsulated cells were then placed in a 0.4% (w/v) chitosan (in 0.1 M acetic acid adjusted to pH 6 with 1 M NaOH) for 10 min. From a previous study, this should result in a chitosan coat of approximately 7 μm thickness.[8] After coating, the capsules were removed by filtration. The produced capsules were then incubated at 37 °C in simulated gastric solution (pH 2 with 1 M HCl, 0.2% (w/v) NaCl, 10 mL) with shaking for 1 h. This was followed by exposure to simulated intestinal solution (6.8% (w/v) KH_2PO_4, pH 7.2 with 1 M NaOH, 50 mL) with shaking at 37 °C for 3 h. Samples were taken at 0, 60, 120, 180, and 240 min and the cells in solution were enumerated by the previously described method. By the 240 min mark, the capsules had completely dissolved. To determine the initial cell concentration, for each experiment a separate 1 mL batch of capsules was taken directly after production and placed into PBS (100 mL) and incubated (1 h, 37 °C). After incubation, the

capsules were placed into a stomacher (Seward stomacher 400 circulator, 250 rpm, 20 min) to ensure their complete dissolution. The initial cell concentration was determined by enumerating the cells in this suspension. Simulated gastric solutions were made to pH 2.0 to represent the low pH found in the nonfasted stomach.[35−37]

Preparation of pHrodo/FITC Labeled *B. breve*. *B. breve* was streaked onto WC agar plates from a previously prepared cell bank and was grown anaerobically (48 h, 37 °C). After growth, the bacteria were inoculated into TPY broth (10 mL) and incubated (37 °C, 22 h) with shaking, during which time the cells grew to ∼9 log(CFU)/mL. After incubation, the cells were centrifuged (3200 rpm, 10 min, 4 °C) and the supernatant was removed before resuspension in phosphate-buffered saline (PBS, pH 9, 10 mL). To this cell suspension, pHrodo succinimidyl ester (1 μL of a 10 mg/mL stock solution in DMSO) was added and conjugation was allowed to proceed in darkness (37 °C, 30 min) with shaking. The cells were then centrifuged (3200 rpm, 10 min, 4 °C) and the supernatant removed before washing with, and resuspending in, PBS (pH 8, 10 mL). This suspension was then centrifuged once more (3200 rpm, 10 min, 4 °C), the supernatant discarded, and the cells resuspended in PBS (pH 7.2, 10 mL), and FITC solution (1 μL of a 10 mg/mL solution in water) was added. The reaction was allowed to proceed in darkness (37 °C, 30 min) with shaking before centrifugation (3200 rpm, 10 min, 4 °C), washing with PBS (pH 7.2, 1 mL), and resuspending in PBS (pH 7.2, 10 mL) to ensure the removal of excess dye. The tube containing the cells was then placed into boiling water (5 min) before switching to ice−water (5 min) to kill the cells and remove any potential for cell division. This was performed in order to reduce the motility of the bacteria when being visualized by microscopy. As the bacteria used are gram-positive and have an extracellular capsule, it is unlikely this treatment led to a large lysis of cells. Additionally, microscopic observation of the post-treated cells gave no indication of this. The suspension was then divided into 1 mL aliquots before centrifugation (13000 rpm, 5 min) and subsequent removal of the supernatant.

Preparation of Alginate-Chitosan Microcapsules Containing pHrodo/FITC Labeled *B. breve*. Alginate solution (2% w/v in water, 1 mL, filtered using Minisart Sterile-R 0.45 μm microfilters) was added to pHrodo/FITC-labeled *B. breve* pellets produced as above and vortexed to ensure complete mixing. This solution was then extruded using a syringe and a pump (2.0 mL/min) into 0.05 M calcium chloride solution (50 mL) and was left to harden for 30 min before filtration. In the case of chitosan-coated alginate microcapsules these were then placed into chitosan solution (0.4% w/v in 0.1 M acetic acid adjusted to pH 6, 10 mL) and left to stand (10 min). These chitosan-coated alginate microcapsules were then removed from the mixture by filtration.

Calibration of Microscope. To extract the pH values from the CLSM images a calibration curve was first constructed. pHrodo/FITC-labeled *B. breve* produced previously was resuspended into PBS (1 mL) that was adjusted accurately to pH 2, 2.5, 3, 4, 5, and 7.2. These new suspensions were placed onto a coverslip and imaged using a Leica SP2 CLSM. Samples were excited with 488 and 546 nm lasers sequentially, corresponding to the excitation wavelengths of FITC and pHrodo, respectively. From these 8-bit images, the pixel intensity of the cells was determined using the onboard software (Leica Confocal Software).

Measurement of pH within Alginate-Chitosan Microcapsules. A single alginate or alginate-chitosan microcapsule containing pHrodo/FITC labeled *B. breve* was placed onto a purpose designed coverslip (consisting of a 50 mm Petri dish with a central section removed which was then replaced with a thin glass coverslip), submerged in simulated gastric solution (pH 2 adjusted with 1 M HCl, 0.2% (w/v) NaCl, 100 μL, 37 °C), and imaged using a CLSM at 488 and 543 nm excitation wavelengths sequentially at 0, 1, 5, 10, 15, 30, 45, and 60 min intervals during incubation at 37 °C. The images were then manipulated using MATLAB (7.11.0) so that the individual pixel intensity could be related to a pH, which was then color coded according to its value to produce "pH maps" of the microcapsules. To do this, first the two images taken at the different excitation wavelengths of the dyes were divided by one another using the Boolean Logic function on the onboard software. This gave each pixel an intensity equivalent to the fluorescence of pHrodo/FITC; these images were then converted to an equivalent matrix of pixel intensities (Figure 1). These intensities were then put into "bins" defined by the range of intensity values equivalent to a known pH, which were then color coded. For example, values in the matrix between 3.3 and 5.8 (equivalent to fluorescence of pHrodo/FITC for pH 6 and 5, respectively) were binned together and assigned the value 20, which was then colored light blue to code for pH 5−6. The values that defined the bins were taken from a previously established calibration curve (Supporting Information).

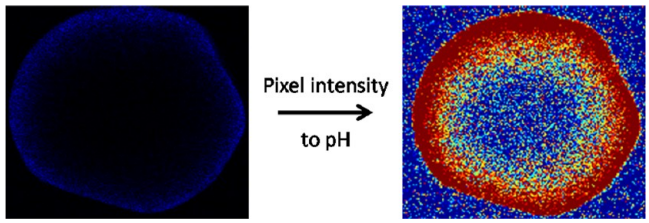

Figure 1. Conversion of pixel intensity to pH. Image on left is produced by the division of the pixel intensities of a picture showing pHrodo fluorescence by the corresponding FITC image. Image on right is the result of coloration of the left image based on the intensity of each pixel.

RESULTS AND DISCUSSION

B. breve was exposed to a range of pHs between 2 and 7 and the viability of the cells measured after 1 h incubation at 37 °C (Figure 2). Gastric emptying time is highly variable, but 1 h was chosen as reasonable residence time of a particulate formulation.[38] There was a steady decrease from 9.3 ± 0.4 log(CFU)/mL to 8.7 ± 0.2 log(CFU)/mL between pH 7 and pH 3, after which the number of culturable cells dropped to ∼4.7 log(CFU)/mL as the pH reached 2.3. At pHs less than or equal to 2, there was no detection of any viable cells (detection limit is 3 log(CFU)/mL). Based on previous research, it is likely that cell death has a kinetic dependency on time in acid.[39] This data shows that this particular probiotic strain is acid-sensitive, showing very low numbers of viable cells at pHs less than 3. The human stomach pH is often lower than this threshold, so these bacteria are unlikely to survive gastric transit.

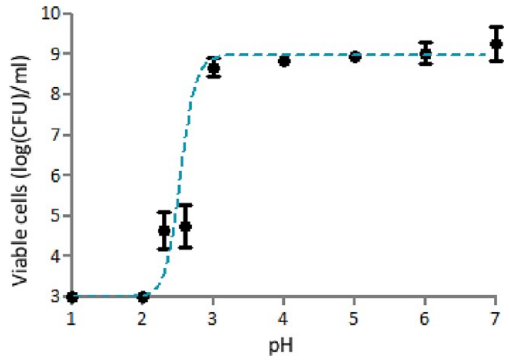

Figure 2. Viability of *B. breve* against TPY medium adjusted to various pH after 1 h incubation at 37 °C; $N = 3 \pm$ standard deviation; limit of detection, 3 log(CFU)/mL; line intended as guide to eye.

Alginate microcapsules have been shown previously to offer a good level of protection to acid sensitive bacteria when exposed

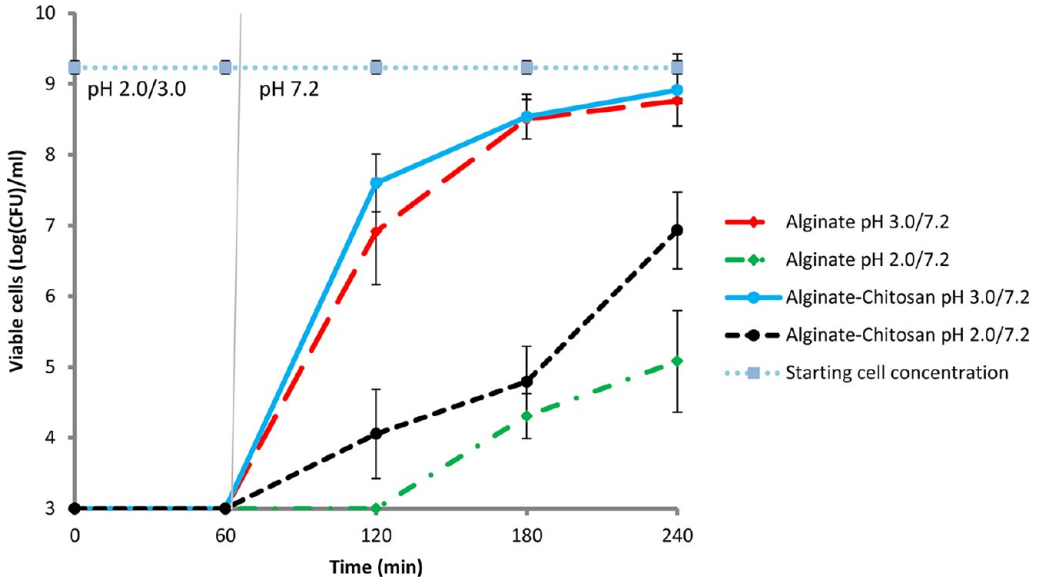

Figure 3. Release of viable cells from alginate and chitosan-coated alginate matrices during exposure to simulated gastric solution (pH 2.0/3.0, 60 min) followed by simulated intestinal solution (180 min) at 37 °C. By the 240 min mark, matrix dissolution was complete. Starting cell concentration included indicating maximum possible survival; $N = 3 \pm$ standard deviation; limit of detection, 3 log(CFU)/mL.

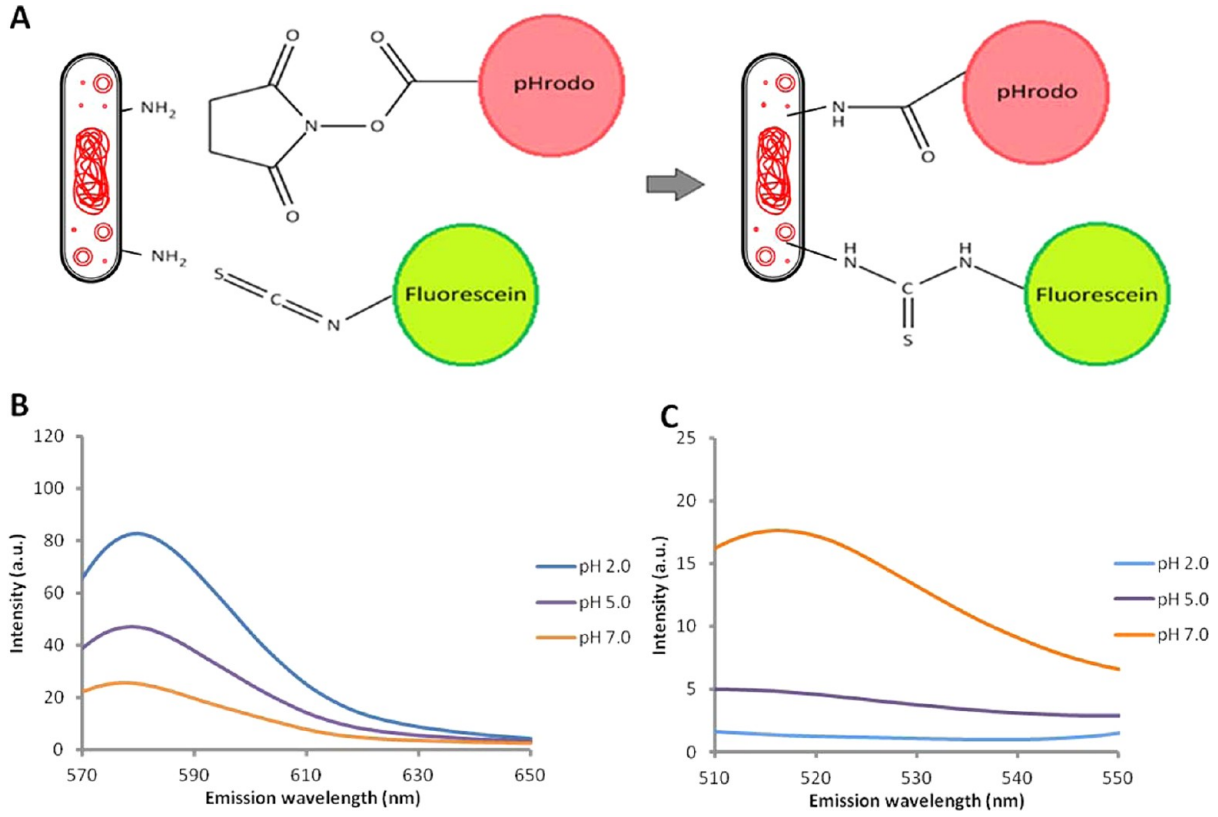

Figure 4. Schematic diagram of dye conjugation to amine moieties within bacteria, producing thiourea and amide moieties when reacting with pHrodo succinimidyl ester and FITC, respectively (A). Fluorescence of pHrodo (B) and FITC (C) when conjugated to *B. breve* showing variation of intensity with pH. For this experiment, a solution of fluorescently labeled *B. breve* conjugate (100 μL) at ~9 log(cells)/mL was diluted into PBS (900 μL) adjusted to pH 2.0, 5.0, and 7.0. The fluorescence of conjugated pHrodo and FITC was then quantified by UV spectrofluorometry (λ_{ex}: 546 and 488, respectively) over the ranges shown. Fluorescence changes with pH are most commonly the result of protonation or deprotonation around a fluorophore's pK_a.[43]

to simulated gastric solutions and coating these matrices with chitosan improves survival further.[7,8,28,30,34,40,41] Our data, shown as release of viable cells to estimate the number of cells that may be deposited in the intestine in vivo, is consistent with these findings (Figure 3). During the first 60 min, no viable cells were detected in the simulated gastric solution of either pH 2.0 or 3.0. The enumeration of *B. breve* in simulated intestinal solution after exposure to pH 3.0 gastric solutions

dx.doi.org/10.1021/bm301569r | *Biomacromolecules* 2013, 14, 387−393

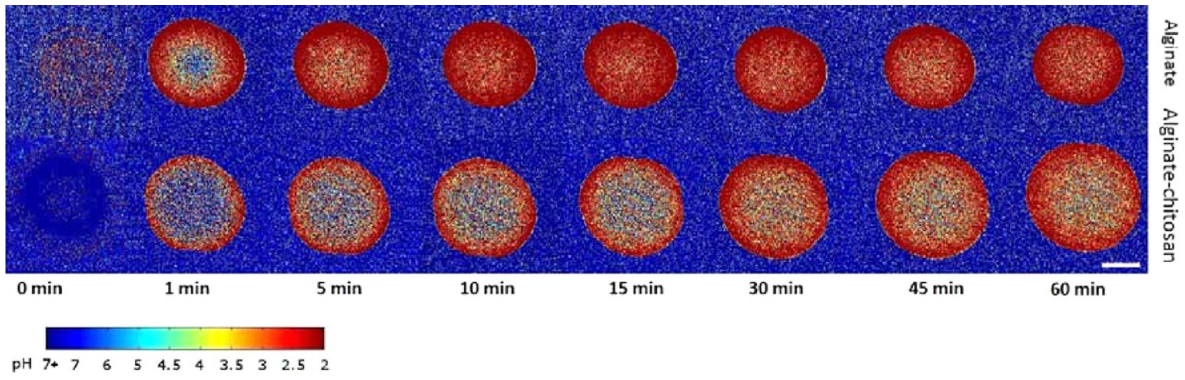

Figure 5. pH maps of an alginate and a chitosan-coated alginate microcapsule during exposure to simulated gastric solution at pH 2.0. Scale: 1 mm.

gave a release of viable cells amounting to 8.7 and 8.9 log(CFU)/mL for alginate and chitosan-coated alginate capsules, respectively (Figure 3). At pH 2, the viable cells released after 240 min amounted to 5.1 and 6.9 log(CFU)/mL for alginate and chitosan-coated alginate capsules, respectively. These values are high, relative to <3 log(CFU)/mL predicted in the control experiment (at pH 2 in Figure 2). The increased survival of cells in the chitosan coated system is believed to be due to an increase in buffering as the acid penetrates the capsule[7] and is also possibly due to reduced porosity at the capsule surface.[42] This provides a demonstration of the efficacy of this encapsulation system in protecting acid-sensitive bacteria. It should also be noted that the release of cells appears slower after exposure to pH 2 solution; this is most likely caused by the death of cells at the periphery first, which leads to a lag associated with the disintegration of the capsule from the extremities first. This would result in the release of the viable cells only once the region containing killed cells had disintegrated.

The pHrodo succinimidyl ester and FITC were conjugated to bacteria via amine residues that were present within the cell (Figure 4A). These dyes were shown to be present by UV−vis spectrofluorometry (λ_{exc}: 488 and 546, for FITC and pHrodo, respectively) and the images showed a change in pixel intensity of the cells when exposed to pH between pH 2 and 7 (Supporting Information). Conjugated pHrodo increased in intensity when the pH was decreased from 7 to 2 (Figure 4B), whereas the fluorescence intensity of FITC decreased (Figure 4C). These cells were then encapsulated within alginate and alginate-chitosan matrices before exposure to simulated gastric solution and visualization by confocal microscopy.

This method allows for the production of "pH maps" of matrices (Figure 5). These maps allow the visualization of the pH as the acid penetrates into the polymer network. This lets the viewer not only see the rate of diffusion of the acid, but also the color-coding, which allows for the identification of specific pH environments within the matrix. It should be noted that cells were killed after labeling to reduce movement during imaging. In the case of alginate capsules, a thick band of red, associated with pHs between 2.5 and 2 appears after only 1 min, accompanied by a clear bright blue region of pH 7−6 in the center of the matrix. As time passes, this central circle can be seen to darken, and the encroachment of the external red band thickens, showing the penetration of acid into the capsule. In the case of chitosan-coated alginate capsules, the appearance of the thick band of red on the perimeter of the capsule is considerably slower and the persistence of higher pH in the center is observably longer than in the uncoated matrices. These images imply a combination of buffering effects, signified by the presence of pH above that of the simulated gastric solution (pH 2), even at the periphery, and a slowing of acid penetration into the polymer network, most likely a result of the formation of an acid-gel. This example demonstrated the ability of our method to produce pH maps and elucidate pH changes occurring within matrices.

To obtain a better view of the pH distribution within the microcapsules, a close comparison of the pH within the matrix after 60 min (from a repeat of the experiment) is shown in Figure 6. In the case of alginate only matrices, there is a thick dark red color, associated with pHs nearing 2.0 around the perimeter of the capsules, in which it would be expected all cells to be dead. In the most part, there is an orange-red color, pertaining to pHs between 2.5 and 3 throughout the rest of the matrix. pHs between 2.3 and 3 correlate to an approximately 4.5 log(CFU)/mL survival of bacteria (based in Figure 2). In the case of alginate encapsulated cells, 60 min exposure to gastric solution resulted in a 5 log(CFU)/mL survival of cells, showing some consistency with our findings (Figure 3), though direct comparison is complicated due to the kinetic dependency of the viability studies. In the alginate-chitosan matrix, a thinner, lighter colored ring of red is seen around the perimeter, most likely due to increased buffering or reduced porosity. Toward the center of the capsules, there is the emergence of yellow and some blue regions associated with pHs up to 5, at which very high cell survival would be seen. This increased pH results in an increase in cell survival, which is seen in the simulated gastric viability assay (Figure 3).

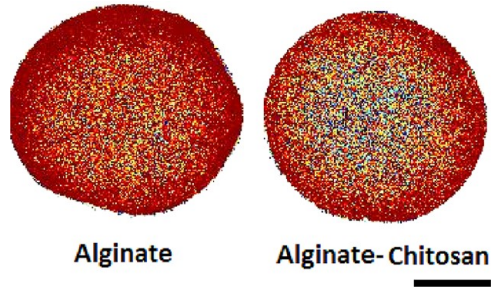

Figure 6. Comparison of pH within alginate and alginate-chitosan matrices after 60 min exposure to simulated gastric juice at pH 2.0 (scale bar: 1 mm). Images taken from a separate experiment to those shown in Figure 5.

dx.doi.org/10.1021/bm301569r | *Biomacromolecules* 2013, 14, 387−393

From the images captured on the confocal microscope it is possible to measure the thickness of the aforementioned ring of red, associated with pHs in the region 2−3, using image analysis software (ImageJ). These pHs should be associated with a relatively rapid cell death according to the viability testing already conducted (Figure 2). The thickness of the red band could then be used to give a representation of encroachment of low pH into the matrix (Figure 7). In both the alginate and chitosan-coated alginate there is a sudden penetration of acid into the periphery of the matrix, which slows over time. This nonlinear behavior is most likely a result of acid-gel formation at the periphery of the capsules during penetration, reducing the rate of diffusion into the matrix. The chitosan-coated alginate matrices seem to slow encroachment of the low pH into the gel, relative to the uncoated samples. The depth of penetration of low pH into the samples measures 367.6 ± 13.4 and 290.4 ± 17.0 μm for the uncoated and chitosan-coated alginate matrices, respectively. This reaffirms the qualitative findings discussed as there is a reduced area of pHs associated with a particularly rapid cell death in the chitosan-coated samples.

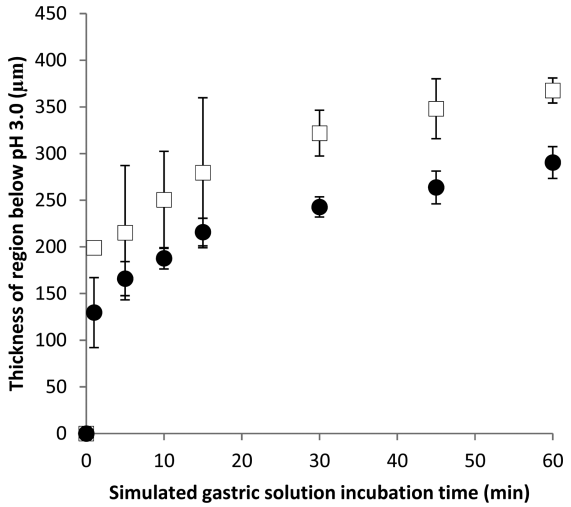

Figure 7. Encroachment of pH < 3.0 into alginate (open squares) and chitosan-coated alginate (closed circles) matrices during incubation in simulated gastric solution at 37 °C; $N = 3 \pm$ standard deviation, band thickness is the average of five measurements at equidistant points on the matrix.

Experimentally, this method is very quick and straightforward. The dyes used may be tailored to provide information at different pH ranges assuming that cell staining dyes with pH dependent fluorescence in this region may be found. There are currently numerous amine-active dyes available at a range of pHs which will allow for higher accuracy at particular pH ranges. Co-staining and pH determination by ratiometric means should make this method resistant to changes in bacterial concentration if it were to be applied with other systems or microbes.

CONCLUDING REMARKS

A method for the reliable visualization of pH within polymer matrices has been developed. This method allows for the production of "pH maps" showing the distribution of pH within a cross-section of a hydrated polymer matrix. This method was then applied to alginate and alginate-chitosan matrices, which are commonly used for the protection of acid-sensitive bacteria. After demonstration of this protective effect in vitro, the pH environment within the matrices was visualized using pH maps. These maps revealed what we suggest to be a combination of buffering, which was seen to increase after coating with the basic chitosan and an encroaching of low pH from the periphery into the matrix rather than a bulk pH change, which slowed with chitosan coating. The use of microbes as carriers of fluorophores for this purpose offers an alternative to free dyes that may otherwise not be retained by the polymer network or the conjugation of dyes to the polymers, which may affect their fluorescence. It is also possible that microparticles could be used as an alternative, such as the polystyrene microparticles with surface-bound dyes used by Sánchez-Martin et al.[44] to measure intracellular pH. There are various studies that use pH-sensitive fluorophores conjugated to polymer particles,[45−47] which could be adapted and evaluated for the observation of pH within porous polymer matrices.

ASSOCIATED CONTENT

Supporting Information

The calibration curve determined for the fluorescence ratio of pHrodo/FITC with pH. This material is available free of charge via the Internet at http://pubs.acs.org.

AUTHOR INFORMATION

Corresponding Author

*E-mail: d.charalampopoulos@reading.ac.uk; v.khutoryanskiy@reading.ac.uk. Tel.: +44 (0) 118 378 8216 (D.C.); +44 (0) 118 378 6119 (V.K.).

Notes

The authors declare no competing financial interest.

ACKNOWLEDGMENTS

This research was supported by Clasado Ltd. and the University of Reading.

REFERENCES

(1) Patrick, G. L. *An Introduction to Medicinal Chemistry*, 1st ed.; Oxford University Press: Oxford, 2005; p 170.
(2) Dea-Ayuela, M. A.; Rama-Iniguez, S.; Torrado-Santiago, S.; Bolas-Fernandez, F. *J. Drug Targeting* **2006**, *14*, 567−75.
(3) Cook, M. T.; Tzortzis, G.; Charalampopoulos, D.; Khutoryanskiy, V. V. *J. Controlled Release* **2012**, *162*, 56−67.
(4) Doherty, S. B.; Auty, M. A.; Stanton, C.; Ross, R. P.; Fitzgerald, G. F.; Brodkorb, A. *Int. Dairy J.* **2012**, *22*, 31−43.
(5) Raffin, R. P.; Colome, L. M.; Guterres, S. S.; Pohlmann, A. R. *Pharm. Dev. Technol.* **2007**, *12*, 463−471.
(6) Ouyang, W.; Chen, H.; Jones, M. L.; Metz, T.; Haque, T.; Martoni, C.; Prakash, S. *J. Pharm. Pharm. Sci.* **2004**, *7*, 315−24.
(7) Graff, S.; Hussain, S.; Chaumeil, J. C.; Charrueaul, C. *Pharm. Res.* **2008**, *25*, 1290−1296.
(8) Cook, M. T.; Tzortzis, G.; Charalampopoulos, D.; Khutoryanskiy, V. V. *Biomacromolecules* **2011**, *12*, 2834−2840.
(9) Ashford, M. *Aulton's Pharmaceutics*, 3rd ed.; Aulton, M. E., Ed.; Elsevier: Amsterdam, 2007; pp 270−286.
(10) Lindström, E.; Chen, D.; Norlén, P.; Andersson, K.; Håkanson, R. *Comp. Biochem. Physiol., Part A: Mol. Integr. Physiol.* **2001**, *128*, 503−511.
(11) Evans, D. F.; Pye, G.; Bramley, R.; Clark, A. G.; Dyson, T. J.; Hardcastle, J. D. *Gut* **1988**, *29*, 1035−1041.
(12) Fordtran, J. S.; Walsh, J. H. *J. Clin. Invest.* **1973**, *52*, 645−657.
(13) Kwiatek, M. A.; Menne, D.; Steingoetter, A.; Goetze, O.; Forras-Kaufman, Z.; Kaufman, E.; Fruehauf, H.; Boesiger, P.; Fried, M.; Schwizer, W.; Fox, M. R. *Am. J. Physiol.* **2009**, *297*, G894−G901.

(14) George, J. D. *Gut* **1968**, *9*, 237−42.
(15) Pygall, S. R.; Whetstone, J.; Timmins, P.; Melia, C. D. *Adv. Drug Delivery Rev.* **2007**, *59*, 1434−52.
(16) Li, L.; Schwendeman, S. P. *J. Controlled Release* **2005**, *101*, 163−173.
(17) Fu, K.; Pack, D. W.; Klibanov, A. M.; Langer, R. *Pharm. Res.* **2000**, *17*, 100−106.
(18) Liu, Y.; Schwendeman, S. P. *Mol. Pharm.* **2012**, *17*, 100−106.
(19) Ding, A. G.; Schwendeman, S. P. *Pharm. Res.* **2008**, *25*, 2041−52.
(20) Ding, A. G.; Shenderova, A.; Schwendeman, S. P. *J. Am. Chem. Soc.* **2006**, *128* (16), 5384−90.
(21) Shenderova, A.; Ding, A. G.; Schwendeman, S. P. *Macromolecules* **2004**, *37*, 10052−10058.
(22) Pygall, S. R.; Kujawinski, S.; Timmins, P.; Melia, C. D. *Int. J. Pharm.* **2009**, *370*, 110−20.
(23) Cope, S. J.; Hibberd, S.; Whetstone, J.; MacRae, R. J.; Melia, C. D. *Pharm. Res.* **2002**, *19*, 1554−63.
(24) O'Connell Motherway, M.; Zomer, A.; Leahy, S. C.; Reunanen, J.; Bottacini, F.; Claesson, M. J.; O'Brien, F.; Flynn, K.; Casey, P. G.; Moreno Munoz, J. A.; Kearney, B.; Houston, A. M.; O'Mahony, C.; Higgins, D. G.; Shanahan, F.; Palva, A.; de Vos, W. M.; Fitzgerald, G. F.; Ventura, M.; O'Toole, P. W.; van Sinderen, D. *Proc. Natl. Acad. Sci. U.S.A.* **2011**, *108*, 11217−22.
(25) Cotter, P. D.; Hill, C. *Microbiol. Mol. Biol. Rev.* **2003**, *67*, 429−53.
(26) Albertini, B.; Vitali, B.; Passerini, N.; Cruciani, F.; Di Sabatino, M.; Rodriguez, L.; Brigidi, P. *Eur. J. Pharm. Sci.* **2010**, *40*, 359−366.
(27) Mazumder, M. A. J.; Burke, N. A. D.; Shen, F.; Potter, M. A.; Stover, H. D. H. *Biomacromolecules* **2009**, *10*, 1365−1373.
(28) Gbassi, G. K.; Vandamme, T.; Ennahar, S.; Marchioni, E. *Int. J. Food Microbiol.* **2009**, *129*, 103−105.
(29) Lin, J. Z.; Yu, W. T.; Liu, X. D.; Xie, H. G.; Wang, W.; Ma, X. J. *J. Biosci. Bioeng.* **2008**, *105*, 660−665.
(30) Liserre, A. M.; Re, M. I.; Franco, B. *Food Biotechnol.* **2007**, *21*, 1−16.
(31) Mandal, S.; Puniya, A. K.; Singh, K. *Int. Dairy J.* **2006**, *16*, 1190−1195.
(32) Krasaekoopt, W.; Bhandari, B.; Deeth, H. *Int. Dairy J.* **2004**, *14*, 737−743.
(33) Chandramouli, V.; Kailasapathy, K.; Peiris, P.; Jones, M. *J. Microbiol. Methods* **2004**, *56*, 27−35.
(34) Krasaekoopt, W.; Bhandari, B.; Deeth, H. C. *Lebensm. Wiss. Technol.* **2006**, *39*, 177−183.
(35) Dressman, J. B.; Berardi, R. R.; Dermentzoglou, L. C.; Russell, T. L.; Schmaltz, S. P.; Barnett, J. L.; Jarvenpaa, K. M. *Pharm. Res.* **1990**, *7*, 756−61.
(36) Mojaverian, P.; Vlasses, P. H.; Kellner, P. E.; Rocci, M. L. *Pharm. Res.* **1988**, *5*, 639−644.
(37) Naguib, M.; Samarkandimb, A. H.; Al-Hattab, Y.; Turkistani, A.; Delvi, M. B.; Riad, W.; Attia, M. *Can. J. Anaesth.* **2001**, *48*, 344−50.
(38) Locatelli, I.; Mrhar, A.; Bogataj, M. *Pharm. Res.* **2009**, *26* (7), 1607−17.
(39) Corcoran, B. M.; Stanton, C.; Fitzgerald, G. F.; Ross, R. P. *Appl. Environ. Microbiol.* **2005**, *71*, 3060−7.
(40) Ding, W. K.; Shah, N. P. *J. Food Sci.* **2009**, *74*, M100−M107.
(41) Hansen, L. T.; Allan-Wojtas, P. M.; Jin, Y. L.; Paulson, A. T. *Food Microbiol.* **2002**, *19*, 35−45.
(42) Gombotz, W. R.; Wee, S. F. *Adv. Drug Delivery Rev.* **1998**, *31*, 267−285.
(43) Hanson, M. A.; Ge, X.; Kostov, Y.; Brorson, K. A.; Moreira, A. R.; Rao, G. *Biotechnol. Bioeng.* **2007**, *97*, 833−841.
(44) Bradley, M.; Alexander, L.; Duncan, K.; Chennaoui, M.; Jones, A. C.; Sánchez-Martín, R. M. *Bioorg. Med. Chem. Lett.* **2008**, *18*, 313−317.
(45) Kobayashi, S.; Kojidani, T.; Osakada, H.; Yamamoto, A.; Yoshimori, T.; Hiraoka, Y.; Haraguchi, T. *Autophagy* **2010**, *6*, 36−45.
(46) Leclerc, L.; Boudard, D.; Pourchez, J.; Forest, V.; Marmuse, L.; Louis, C.; Bin, V.; Palle, S.; Grosseau, P.; Bernache-Assollant, D. *J. Nanopart. Res.* **2012**, *14*, 1−13.
(47) Hornig, S.; Biskup, C.; Gräfe, A.; Wotschadlo, J.; Liebert, T.; Mohr, G. J.; Heinze, T. *Soft Matter* **2008**, *4*, 1169−1172.